Environmental and Experimental Botany 172 (2020) 104000

Contents lists available at ScienceDirect

Environmental and Experimental Botany

journal homepage: www.elsevier.com/locate/envexpbot

Dark septate endophyte enhances maize cadmium (Cd) tolerance by the remodeled host cell walls and the altered Cd subcellular distribution

Mi Shen[a,1], Harald Schneider[b,1], Runbing Xu[a], Guanhua Cao[c], Hanbo Zhang[a], Tao Li[a,*], Zhiwei Zhao[a,*]

[a] State Key Laboratory for Conservation and Utilization of Bio-Resources in Yunnan, Yunnan University, Kunming, 650091, Yunnan, PR China
[b] Center of Integrated Conservation, Xishuangbanna Tropical Botanical Garden, Chinese Academy of Sciences, Menglun Township, 666303, Yunnan, PR China
[c] School of Traditional Chinese Medicine, Yunnan University of Traditional Chinese Medicine, Kunming, 650500, Yunnan, PR China

ARTICLE INFO

Keywords:
Dark septate endophyte (DSE)
Exophiala pisciphila
Maize (*Zea mays*)
Cell wall
Cadmium tolerance mechanism

ABSTRACT

Evidence accumulated in recent years supports the crucial role of remodeled cell walls (CWs) in enabling plants to adapt to environmental challenges. However, the metal tolerance and alleviation mechanisms involving the CWs by endophyte-plant interactions to toxic metals have not yet been elucidated. In the present study, these mechanisms are tested by exploring the maize (*Zea mays*) Cd tolerance by modifying its root CW structure via inoculation with a dark septate endophyte (DSE) fungus *Exophiala pisciphila*. Our present study demonstrates that the root CWs were the primary site for Cd accumulation, functioning as a sink for toxic Cd ions. Interestingly, *E. pisciphila* colonization significantly bioaugmented subcellular compartmentalization of maize roots and increased the Cd content of various CW subfractions through a significantly increased enzyme activity, e.g., pectin methylesterase, as well as an upregulated expression of genes involved in CW biosynthesis and changes in the contents of functional groups in pectin and hemicellulose 1 in response to Cd stress. Consequently, the enhanced Cd compartmentation in plant CWs by DSE lowers the entry of trace metals in the protoplast, thereby conferring the tolerant races of plants that can survive and thrive on metal-contaminated soils.

1. Introduction

Going beyond the traditional knowledge of the mechanical support to the plant body, the more functional aspects of plant cell walls (CWs), a distinguishing trait from animal cells, have intrigued investigators, where numerous complex physicochemical and enzymatic processes take place (Voxeur and Hofte, 2016). Recently, as the first structure of plant cells to come in contact with trace metals, the binding properties of the CWs as a mechanism of metal tolerance in plants, e.g. accumulating toxic metal cations, are attracting increasing attention (Parrotta et al., 2015; Berni et al., 2019). A comparative study on the Pb accumulation and detoxification between in the mining and non-mining ecotypes of *Athyrium wardii*, one of the dominant plant species flourishing on the Pb–Zn mine tailings in China, shows that CW deposition and vacuolar compartmentalization are the important adapted Pb detoxification mechanisms of the mining ecotype, which ensured it adapt well to growing in extremely Pb-polluted habitats (Zhao et al., 2015). Also, a case study of newly identified Cd hyperaccumulator, *Sedum plumbizincicola*, further confirmed the crucial role of CWs in Cd storage in the process of evolution, hence contributing to its hyperaccumulation and hypertolerance (Peng et al., 2017). Subsequently, numerous reports show that root CWs have important chemical characteristics in algae, bryophytes, pteridophytes, and various seed plants (gymnosperms, monocotyledons, and dicotyledons), for instance, various functional groups (e.g., carboxyl, hydroxyl) deriving from the different wall polysaccharides favors ion-exchange mechanisms with wall counterions, which make it a very good biosorbent of trace metals (Parrotta et al., 2015), e.g. 80–87 % of the accumulated Pb bound to the CWs in *Potamogeton crispus* (Qiao et al., 2015). Recently, Xia et al. (2018) report that wall-associated kinase gene *OsWAK11* alleviates the phytotoxicity of excess copper in rice by regulating the methylesterification of the cell wall. Prevailing evidence from both physiological, proteomic and transcriptome data also supports the ion retention in the functional CWs seems to be the first strategy in response to metal entry in diverse plants (Fernandez et al., 2014; Zhang et al., 2017; Kollárová et al., 2019; Lan et al., 2019; Yang et al., 2018).

On the other hand, the CW is in its turn affected by trace metals, since both its biosynthesis and composition, characterized by proteins,

* Corresponding authors.
E-mail addresses: litao@ynu.edu.cn (T. Li), zhaozhw@ynu.edu.cn (Z. Zhao).
[1] These authors contributed to this work equally.

https://doi.org/10.1016/j.envexpbot.2020.104000
Received 9 October 2019; Received in revised form 21 December 2019; Accepted 3 January 2020
Available online 30 January 2020
0098-8472/

polysaccharides and in some instances lignin and other phenolic compounds, conferring the ability to bind non-covalently and/or covalently trace metals via functional groups, can be altered (Xiong et al., 2009; Douchiche et al., 2010; Krzesłowska et al., 2019). Recently, Zhang et al. (2019a) reports that the altered root CW components e.g. the increased neutral sugar and uronic acid of pectin, hemicellulose 1, hemicellulose 2 and cellulose, and the enhanced carboxyl groups of pectin and hemicellulose 2 with more metal-binding sites, confer the remarkable tolerance of tall fescue (*Festuca arundinacea*) to Pb^{2+} stress. And the CW remodeling process is regulated by CW-related enzymes, e.g. the enhanced Cd absorption and fixation to lignified CWs via the activity of cinnamyl alcohol dehydrogenase (Qiu et al., 2018). Although a cascade of evidence emphasizes the functional roles of the remodeling CWs in the plant tolerance in abiotic stress, e.g. metal pollution, the tolerance and alleviation mechanisms involved in the bioaugmented accumulation of metal ions in CWs by diverse root-associated endophytic bacteria and fungi, including the most ubiquitous mycorrhizal fungi and DSEs, have not yet been elucidated (Shi et al., 2019; Zhang et al., 2019b).

For a plant in its natural context, diverse endophytic fungi, found in all plant species examined to date, have been shown to be essential for the plant survival, adaptation, and tolerance in metal-polluted mine soil, as well as in optimizing the plant and its associated microorganisms for phytoremediation (Hou et al., 2017; Thijs et al., 2016). Subsequently, several reports further confirm the vital role of the modifications in the physicochemical properties of CWs in trace metal response of plants, as well in protecting the host against disease, improving plant nutrition and promoting growth (Thavamani et al., 2017; Shi et al., 2019). A similar strategy has been suggested previously for the model plant maize in the presence of a dark septate endophytic fungus (DSE), one of the most common fungal colonizers of roots (Wang et al., 2016). We found, for example, the promoted maize growth *via* DSE colonization with the altered subcellular compartmentalization of 51.0 % and 55.8 % Cd accumulated in leaf and root CWs, compared to the reduced values of 38.6 % and 37.2 % in the non-DSE colonized controls, under 100 mg kg^{-1} Cd stress (Wang et al., 2016). In the current study, *Exophiala pisciphila*, a dominant root-associated DSE fungus in an old multiple-metal mine smelting site, SW China, was targeted as the fungal inoculant, and maize (*Zea mays*), a key plant for bio-energy and phytoremediation of toxic metals from contaminated soil (Thewys et al., 2010; Moreira et al., 2016), was used as phytoremediation plants, and the mechanisms of enhanced trace metal binding in maize root CWs by *E. pisciphila* were comprehensively elaborated. We hypothesize that DSE inoculation alleviates the phytotoxicity of excess Cd in maize by the enhanced sequestration of metals in specific intracellular compartments e.g. the repartitioned Cd in the various CW subfractions, via triggering the related-CW enzymes and by the increased transcriptional regulation of CW synthesis. The novelty of our research is the first analysis characterizing the specific physiological, biochemical and molecular actions of plant CWs bioaugmented by their root-associated endophyte to toxic Cd stress. This model allows us to develop and validate new hypotheses about the functional roles of cell wall remodeling towards an enhanced understanding of plant–microbiome interactions to improve phytoremediation.

2. Materials and methods

2.1. Biological materials

E. pisciphila H93 (accession number ACCC32496, preserved in the Agricultural Culture Collection of China), one of the dominant root colonizers in an old multiple-metal mine smelting site, SW China, was used as the fungal inoculant (Zhang et al., 2013), which enhanced the metal resistance of plants via the bioaugmented accumulation of metal ions in the CWs (Wang et al., 2016). Maize (*Zea mays*) B73, a model plant, was selected as the host (Schnable et al., 2009; Slycken et al., 2013). To obtain sterile seedlings, uniformly sized seeds were selected, surface-sterilized and germinated as previously described (Wang et al., 2016). Then, the germinated seeds were transplanted into 250 mL Erlenmeyer flasks (one seed per flask) containing 10 mL of sterile water and cultured with a 16/8 h light/dark cycle at 25/22 °C for 3 days. Finally, the uniform seedlings were targeted for the following experiments.

2.2. Experimental design

Half of the 3-day seedlings were inoculated with two fungal disks (diameter of 0.5 cm) cut from a fresh culture of *E. pisciphila* (14 days) per flask. The other half of the seedlings, which were the negative controls, were inoculated using equally sized sterile hyphae (autoclaved for 2 h at 121 °C). One week later, the running DSE hyphae but microsclerotia successfully colonized the roots of the DSE-inoculated seedling. And then both the noninoculated and DSE-inoculated maize plants (10-day seedlings) were randomly divided into two groups and supplemented with either 0 or 22.4 mg kg^{-1} Cd ($3CdSO_4{\cdot}8H_2O$ added into 1/2 Hoagland's solution), which significantly inhibited the maize growth, but not for the fungal inoculant (Li et al., 2011). Thus, four treatments in total were conducted, i.e., DSE-inoculated (Cd_DSE) and noninoculated maize (Cd_nDSE) under Cd stress, and maize with DSE (nCd_DSE) and noninoculated maize (nCd_nDSE) with no Cd supplements. Then, all maize seedlings were cultured in 250 mL Erlenmeyer flasks containing half-strength Hoagland's solution with a 16/8 h light/dark cycle at 25/22 °C for 3 weeks in a culture chamber. During the growth period, the nutrient solution was renewed to a maximum volume of 200 mL every two days using 1/2 Hoagland solution without additional Cd supplements. Finally, the 31-day maize seedlings from all 4 treatments were collected, when the most typical colonization of microsclerotia occurred in the roots of DSE-inoculated maize. The roots and shoots were harvested separately and washed thoroughly with deionized water. And DSE colonization intensity was evaluated using the gridline intersect method (Li et al., 2011). The cadmium adhered to the root surface was removed with 10 mM $CaCl_2$ at 4 °C for 10 min. Each treatment was conducted with 4 replicates.

2.3. Cell wall and its subfraction extraction and Cd concentration determination

Fresh root tips of both Cd_nDSE and Cd_DSE seedlings were harvested, then homogenized to powder and used for the extraction of CW materials, as described by Zhong and Lauchli (1993). The final freeze-dried pellet was collected and weighed as the crude CWs and used subsequently for the extraction of CW subfractions and the determination of Cd concentrations. Firstly, the total crude CWs were treated twice in a boiling water bath for 1 h using 0.5 % ammonium oxalate buffer (containing 0.1 % NaBH4, pH = 4). After centrifugation for 5 min at 10 000 × *g*, the two supernatants were pooled and marked as pectin fraction. Subsequently, the pellets were extracted three times with 4 % KOH (containing 0.1 % NaBH4) at room temperature for 24 h, and the pooled supernatants were assigned as hemicellulose 1. And then the remaining pellets were similarly subjected to triple extractions with 24 % KOH (containing 0.1 % NaBH4), and finally yielded hemicellulose 2, and others (e.g., cellulose, lignin, and proteins) (Zhong and Lauchli, 1993).

The Cd accumulated in the CWs, the non-CW fractions (i.e., the pooled supernatants) and 4 CW subfractions was evaluated. First, the above materials were wet digested in a 5 ml mixture of strong HNO_3: $HClO_4$ (4: 1, v/v). The Cd content was determined via atomic absorption spectrophotometry (Shimadzu, AA-6300, Japan). Standard reference material of poplar leaves (GBW 07604, National Research Center for Certified Reference Materials, China) was used as a part of the quality control protocol (accuracies within 100 ± 20 %) (Wang et al., 2016).

2.4. Characterization of functional groups in root CWs and CW subfractions

The characterization of functional groups in the root CWs and 4 CW subfractions were assessed using Fourier transform infrared (FTIR) spectroscopy. First, the root CWs and their subfraction powders (2 mg) were mixed with 200 mg of KBr as the background material (Wu et al., 2015), and then pressed into thin slices. A Fourier transform infrared spectrometer (NicoletiS10, USA) was used to identify the functional groups involved in metal ion biosorption in CWs within the range of $4000-400\ cm^{-1}$.

2.5. Assaying the activity of CW-related enzymes

The total activity of the 3 key enzymes related to CW metabolism, i.e., PME (pectin methylesterase), PAL (phenylalanine ammonialyase), and CWP (cell wall peroxidase), were assessed at 4 °C. Firstly, 200 mg fresh root samples were weighted and homogenized in 1.5 mL of 0.1 M sodium phosphate buffer (pH = 7.5). After centrifugation for 10 min at 15 000*g*, the pellet was homogenized for 2 h in 1.5 mL of 0.1 M sodium phosphate buffer (pH = 7.5, containing 1 M NaCl, 5 mM β-mercaptoethanol and 0.05 % (v/v) protease inhibitor (Sigma)), then centrifuged and the supernatant was filtered and the retained proteins were collected and used for the determination of total PME activity as described by Muschitz et al. (2015). According to the description by Cahill and Mccomb (1992), 300 mg root tissue was ground with liquid nitrogen and homogenized in 4 ml of 0.1 M Tris/HCl buffer (pH = 8.9, containing 10 mM mercaptoethanol) and then centrifuged at 15 000*g* for 30 min at 4 °C. The supernatant was collected and used for the determination of total PAL activity. As for the determination of CWP activity, the root samples were initially ground with liquid nitrogen and homogenized in ice-cold buffer (50 mM sodium succinate, 10 mM calcium chloride, 1 mM dithiothreitol) at a ratio of 10: 1 buffer to sample fresh weight. After centrifugation at 2000*g* for 5 min, the pellet was collected and washed twice in 50 mM sodium succinate to remove cytoplasmic peroxidase activity. Finally, the pellet was resuspended and the total activity of CWP was assayed as described by Bacon et al. (1997). The total activity of CW-related enzymes were evaluated using assay kits for PME (GMS16038.1, USA) and for PAL and CWP (Nanjing Jiancheng Bioengineering Institute, China) according to the manufacturer's protocols. Four replicates were conducted for each treatment.

2.6. RNA-seq assay for the expression of CW-related genes

The root samples of the 4 treatments were collected, and the total RNAs were extracted using the RNeasy Plant Mini Kit (QIAGEN, Hilden, Germany). The concentration and integrity of RNA samples were evaluated, and the RNA samples with integrity values over 6.5 were used for the following cDNA library construction and sequencing. A total of 3 biological replicates were conducted for each treatment.

The cDNA libraries were prepared using the TruSeq Sample Preparation Kit (Illumina). Library quality was assessed on the Agilent Bioanalyzer 2100 system. Paired-end sequencing with 150 bp was performed using an Illumina HiSeq 4000 instrument (Illumina). The RNA-Seq dataset has been deposited in the NCBI SRA with accession PRJNA506746. After removing reads containing adapter, ploy-N, and low-quality reads, clean reads were obtained and mapped to the maize B73 genome (downloaded from ftp://ftp.ensemblgenomes.org/pub/release-30/plants/fasta/zea_mays/dna/) (Schnable et al., 2009) built by Bowtie v2.2 by TopHat v2.0.12. Then, the uniquely mapped reads were counted using intersectBed in the BEDTools package (Quinlan and Hall, 2010), and all subsequent analyses were based on the uniquely mapped reads.

HTSeq v0.6.1 was used to count the numbers of RNA-seq reads that were uniquely mapped in the maize genome (Anders et al., 2015), and then the FPKM (expected number of Fragments Per Kilobase of transcript sequence per Million base pairs sequenced) of each gene was calculated (Trapnell et al., 2010). The expression genes of maize were annotated from the B73 genome (Schnable et al., 2009).

Differential expression analysis among the 4 treatments was performed by the DESeq R package version 1.18.1 using a model based on the negative binomial distribution. The resulting p-values were adjusted using the Benjamini and Hochberg's approach for controlling the false discovery rate. Differentially expressed genes (DEGs) were assigned with an adjusted p-value < 0.05.

To characterize the DEGs related to CW, GO and KEGG enrichment analyses were conducted. GO enrichment analysis of DEGs was implemented by the GO seq R package, in which the gene length bias was corrected. KOBAS (2.0) software was used to test the statistical enrichment of DEGs in KEGG pathways (http://www.genome.jp/kegg/). Both significantly enriched GO terms and KEGG pathways with a corrected p-value < 0.05 were evaluated.

2.7. Quantitative real-time PCR validation

To verify the RNA-seq results, 15 genes were randomly selected, and qRT-PCR with three independent biological replicates for each treatment was conducted using the specific primer pairs amplifying 100–150 bp (Table S1). qRT-PCR was performed on an Applied Biosystems 7500 Real-Time PCR system (Applied Biosystems, CA, USA) using SYBR Premix Ex Taq (Takara, Japan). The most stable 18S rRNA gene of maize was used as an internal control (Chen et al., 2012), and the relative quantification of specific mRNA levels was performed using the comparative the $2^{-\Delta\Delta Ct}$ method. Pearson correlation analysis of DEG expression was performed between the transcriptome and qRT-PCR.

2.8. Statistical analysis

IBM SPSS Statistics 22.0 software was used for data analysis. Prior to statistical analysis, normality and homogeneity of variances were confirmed using the Shapiro-Wilkson test and Levene statistics, respectively. Data on the biomass and the activity of 3 CW-related enzymes were subjected to a two-way analysis of variance (ANOVA) followed by post hoc tests using Bonferroni corrections to detect significant differences among the DSE-inoculated and Cd addition treatments as well as the two-factor interaction. Differences in the Cd proportions and concentrations in the CWs and CW subfractions between the maize inoculated with *E. pisciphila* and the noninoculated treatments, and in the DSE-colonization intensity between the DSE-inoculated maize treatments under 0 and 22.4 mg kg^{-1} Cd stress were compared using a Student's *t*-test. All data are represented as means ± SD.

3. Results

3.1. Cadmium localization in maize root cells

All inoculated treatments were successfully colonized by *E. pisciphila*, with a 33.8 % and 56.2 % colonization intensity under 0 and 22.4 mg kg^{-1} Cd stress, respectively (Fig. S1). Two-way ANOVA results showed that the maize growth (both roots and shoots) was significantly affected by both Cd and DSE-inoculation as well as a significant interaction between Cd and DSE-inoculation, except for the insignificant effects of two-factor interaction on maize shoots (Table S2). Compared to the noninoculated controls, inoculation of *E. pisciphila* alleviated the toxicity of excessive Cd in the substrates and significantly promoted the growth of maize (Fig. S2).

Inoculated accessions showed an increased Cd accumulation of 953.4 ± 100.2 mg kg^{-1} in the root CWs compared to 717.5 ± 112.1 mg kg^{-1} in the noninoculated controls. The proportion of Cd accumulated in the CWs increased from 56.9 % in the controls to 85.0 % in the inoculated plants (Fig. 1). Consequently, the enhanced Cd

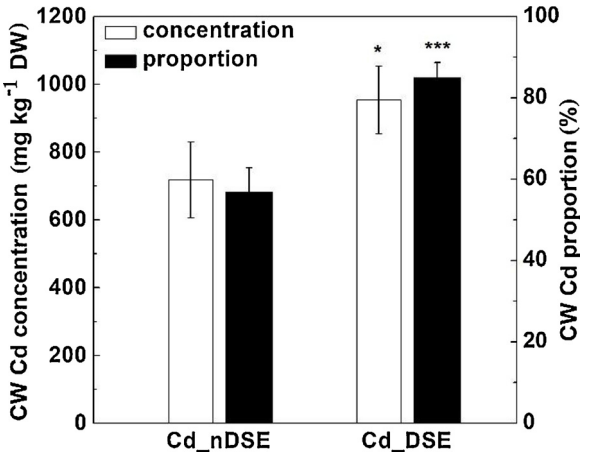

Fig. 1. Cd concentrations and proportions in the root CWs of maize both noninoculated (Cd_nDSE) and inoculated (Cd_DSE) with *E. pisciphila* under 22.4 mg kg^{-1} Cd stress for 3 weeks. The data are presented means ± SD (n = 4), and asterisks indicate significant differences between treatments (* $p < 0.05$, *** $p < 0.001$).

accumulation by cell walls further restricted the translocation of Cd from roots to shoots, and there was little change in shoot Cd concentrations between the DSE-inoculated maize (366.0 ± 22.5 mg kg^{-1}) and the noninoculated controls (360.4 ± 30.2 mg kg^{-1}), although DSE-maize roots accumulated far more Cd (1116.9 ± 67.1 mg kg^{-1}) than that in controls (788.5 ± 133.8 mg kg^{-1}) (Fig. S3).

Compared to the noninoculated maize, inoculation of *E. pisciphila* increased the accumulation of Cd in all 4 CW subfractions, especially for the significantly increased Cd in pectin and hemicellulose 1 (Table 1). However, we noted that the colonization of *E. pisciphila* significantly decreased the Cd proportion in hemicellulose 2 and the other subfractions but increased the Cd proportion in pectin and hemicellulose 1 (Table 1).

The CW spectra obtained via FTIR spectroscopy revealed several differences in the absorption peaks associated with inoculation with DSE. Specifically, the peak positions that were especially affected were the polysaccharide chain (approximately 1059 cm^{-1}) and the sulfate/phosphate (approximately 1245 cm^{-1}) groups in pectin and the hydroxyl/amine (approximately 3413 cm^{-1}), carboxyl (approximately 1378 cm^{-1}), and polysaccharide chain (approximately 1059 cm^{-1}) groups in hemicellulose 1 (Fig. S4).

3.2. Effects of DSE inoculation on the activity of key enzymes involved in CW metabolism

Analysis by two-way ANOVA showed significant effects of DSE-inoculation and Cd stress but the interaction between DSE-inoculation and Cd stress on the activity of three CW-associated enzymes, namely, PME, PAL, and CWP (Table 2). Compared to the noninoculated controls, inoculation with *E. pisciphila* significantly increased the activity of all three CW-associated enzymes surveyed in the roots of maize under Cd stress ($p < 0.05$) (Fig. 2). While, there was only a slight increase in the CW-associated enzymes between the DSE- and noninoculated treatments under no Cd stress ($p > 0.05$), except for the enhanced CWP activity. Interestingly, both PAL and PME, showed inhibited activity in response to Cd stress, whereas CWP showed increased activity. This response to Cd stress was observed in both accessions inoculated with DSE and the noninoculated controls. DSE inoculation did not completely alleviate the negative inhibition of toxic Cd stress on PAL and PME, even compared with maize grown without Cd supplements (Fig. 2).

Table 2
A two-way ANOVA for effects of DSE-inoculation, Cd supplements and their interaction on the activity of 3 cell wall-related enzymes in the maize roots.

Source of variation	SS	d.f.	MS	*F*	P
PME					
Cd	4.569	1	4.569	28.114	0.000***
DSE	2.364	1	2.364	14.546	0.002**
Cd*DSE	0.005	1	0.005	0.032	0.860
Error	1.950	12	0.163		
Total	131.821	16			
PAL					
Cd	40.421	1	40.421	10.361	0.007**
DSE	19.845	1	19.845	5.087	0.044*
Cd*DSE	0.421	1	0.421	0.108	0.748
Error	46.816	12	3.901		
Total	1295.701	16			
CWP					
Cd	0.234	1	0.234	109.703	0.000***
DSE	0.063	1	0.063	29.537	0.000***
Cd*DSE	4.807E-07	1	4.807E-07	0.000	0.988
Error	0.026	12	0.002		
Total	4.783	16			

3.3. RNA-seq analyses of the four experimental setups

The four RNA transcript profiles—nCd + nDSE, nCd + DSE, Cd + nDSE, Cd + DSE—yielded in total 99,214,582 to 152,879,754 clean reads including the three replicates for each of the four treatments. In total, each sample included over 14 Gb of RNA-seq data, of which 76.43 %–85.69 % were uniquely mapped to the maize reference genome sequence (Table S3). The FPKM normalized data employed to quantify the gene expression level were highly reproducible among the three replicates conducted for each of the four biological meaningful treatments, with Pearson coefficients between 0.953 and 0.986 (Fig. S5). The qRT-PCR validation of 15 randomly selected genes from the DEGs identified in the four comparisons showed a strong correlation with the deep sequencing results (r^2 = 0.9029, Fig. S6).

3.4. DEGs in response to Cd stress and DSE inoculation

In total, 8,643 DEGs were identified in the four comparisons, namely, the two pairs to explore the Cd stress response nCd + nDSE v. Cd + nDSE and nCd + DSE v. Cd + DSE and the two pairs to explore

Table 1
Cd concentrations (above slash) and the proportions (below slash) of Cd accumulated in the different CW subfractions of maize roots inoculated or noninoculated with *E. pisciphila* under 22.4 mg kg^{-1} Cd stress. The data are presented as the means ± SD (n = 4), and asterisks indicate significant differences between treatments (** $p < 0.01$, *** $p < 0.001$).

Treatments	Cd concentration (mg kg^{-1}) and proportion (%)			
	Pectin	Hemicellulose 1	Hemicellulose 2	Others
Cd_nDSE	64.39 ± 14.63 / 8.92 ± 0.94	174.11 ± 39.81 / 24.10 ± 2.51	137.14 ± 16.50 / 19.38 ± 2.93	341.85 ± 56.40 / 47.60 ± 1.70
Cd_DSE	135.72 ± 12.18***/14.34 ± 1.90**	297.41 ± 14.66**/ 31.35 ± 2.24**	161.33 ± 30.63 / 16.86 ± 2.18	358.94 ± 65.69 / 37.45 ± 2.92**

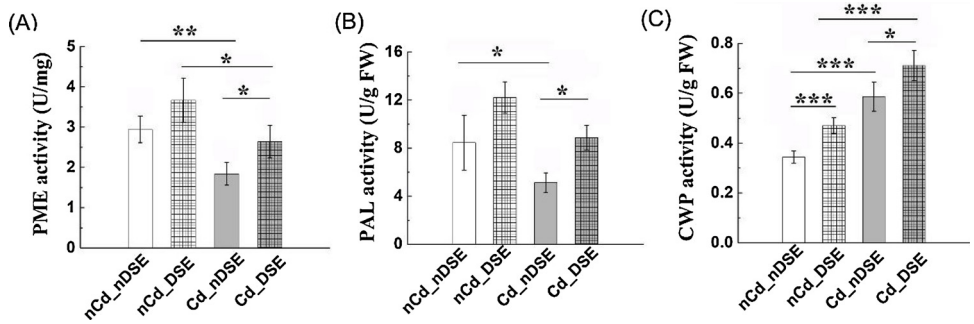

Fig. 2. PME (A), PAL (B), and CWP (C) activity in the root CWs of maize inoculated or noninoculated with *E. pisciphila* under 0 and 22.4 mg kg^{-1} Cd stress for 3 weeks.

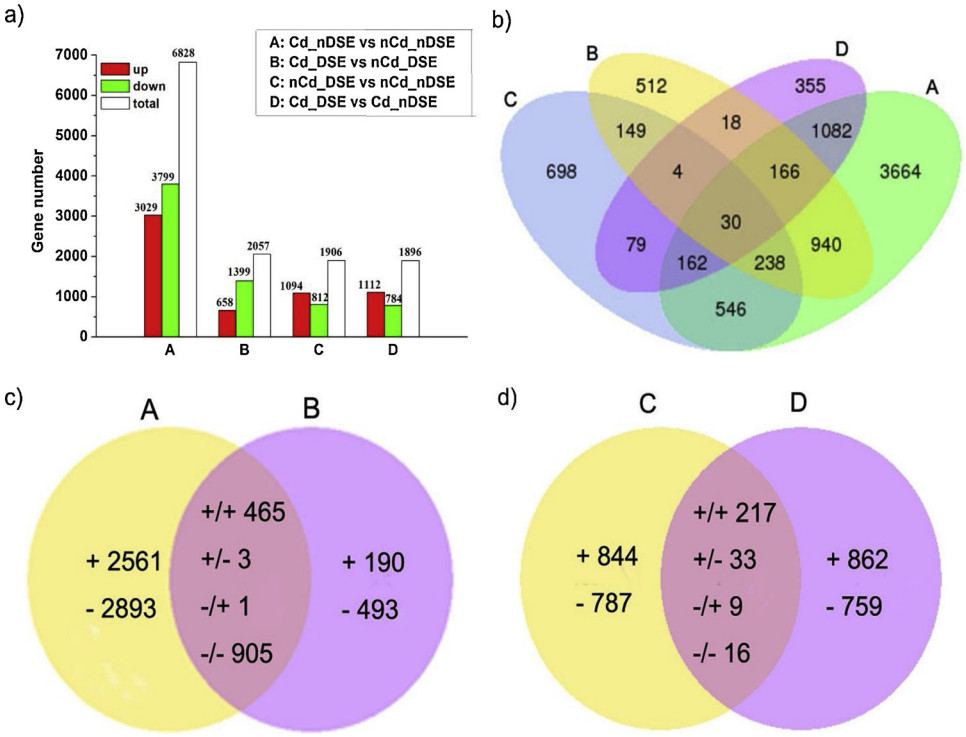

Fig. 3. Venn diagrams of DEGs in maize roots inoculated and noninoculated with *E. pisciphila* under 0 and 22.4 mg kg^{-1} Cd stress for 3 weeks. +, upregulated; −, downregulated; +/+, upregulated in overlap; −/−, downregulated in overlap; +/−, upregulated in left treatments and downregulated in right treatments; −/+, downregulated in left treatments and upregulated in right treatments.

the DSE inoculation response nCd + nDSE v. nCd + DSE and Cd + nDS v. Cd + DSE Fig. 3a and b. In total, 6,828 Cd-responsive DEGs were found in the Cd stress response without DSE nCd + nDSE v. Cd + nDSE. Of these, 3,029 were upregulated, and 3,799 were downregulated. The amount of DEGs was reduced to 2057 Cd-responsive DEGs in those samples with DSE nCd + DSE v. Cd + DSE, of which 658 were upregulated and 1,399 downregulated Fig. 3a and c. In contrast, DSE treatment did not result in such a strong difference in the number of DEGs, with 1,906 DSE-responsive DEGs without Cd treatment nCd + nDSE v. nCd + DSE and 1,896 DSE-responsive DEGs with Cd treatment Cd + nDS v. Cd + DSE Fig. 3a and d). In total, 1374 DEGs were regulated exclusively by Cd exposure and 275 DEGs by DSE inoculation (Fig. 3c and d).

Some notable differences existed in the response of DEGs to different treatments. 465 DEGs (33.8 %) were upregulated by Cd exposure alone, whereas 217 DEGs (78.9 %) were upregulated by DSE inoculation alone. Conversely, 905 DEGs (65.8 %) were downregulated by Cd exposure without DSE, but only 16 DEGs (5.82 %) were downregulated in roots of DSE-colonized maize. Only a small number of overlapping expression patterns were present in the different Cd and DSE responses, namely, 4 (0.29 %) and 42 (15.27 %), respectively (Fig. 3c and d).

3.5. Identification of genes and metabolic pathways

The four carried comparisons recovered between 79 and 257 significantly enriched GO terms—nCd + nDSE v. Cd + nDSE = 257, nCd + DSE v. Cd + DSE = 121, nCd + nDSE v. nCd + DSE = 79, Cd + nDS v. Cd + DSE = 189 (Table S4). For Cd-responsive upregulated DEGs, 309 and 252 GO terms were significantly enriched in the comparison between the non-DSE and DSE treatments, respectively. For the Cd-responsive downregulated DEGs, 144 and 41 significantly enriched GO terms were found. For the DSE-responsive upregulated DEGs, 132 and 129 significantly enriched GO terms were found, whereas the DSE-responsive downregulated DEGs showed 1 and 126 significantly enriched GO terms (Table S4).

Among those, 32 significant GO terms were associated with CW metabolism. Twenty-two DEGs significantly enriched in GO terms were shared between the Cd-responsive and DSE-responsive DEGs, whereas 7 were limited to downregulated Cd-responsive DEGs and 3 limited to upregulated DSE-responsive DEGs. Of these shared DEGs, 8 were involved in CW organization and plant-type CW biogenesis, 6 were involved in lignin and its monomers biosynthesis (e.g., PAL, CWP, and PME), 4 were involved in the hemicellulose metabolisms (such as xyloglucan and xylan metabolic processes), and 4 were involved in other

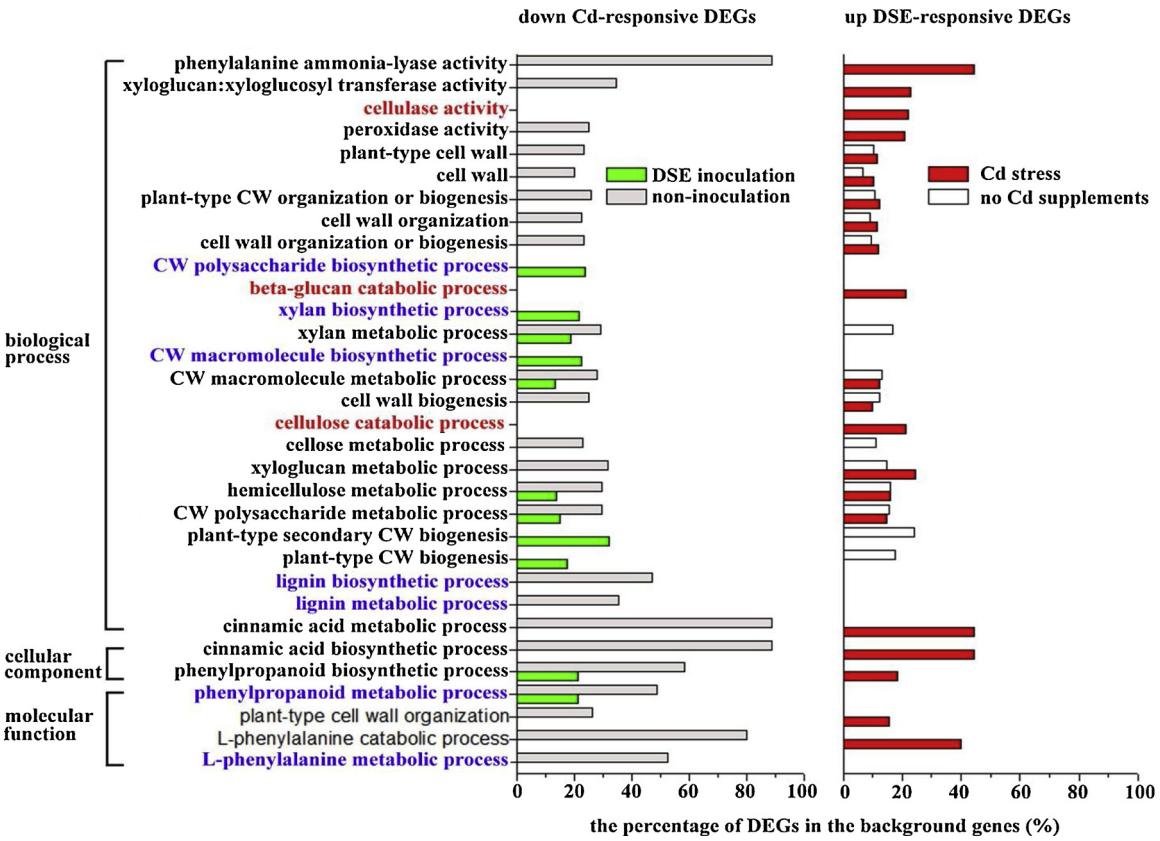

Fig. 4. GO significant enrichment analysis related to CW metabolism from the downregulated Cd-responsive and upregulated DSE-inoculated DEGs. GO terms labeled with blue and red fonts represent significant enrichment by downregulated Cd-responsive DEGs alone and by upregulated DSE-inoculated DEGs alone, respectively.

CW biosynthesis processes, such as plant-type secondary CW biogenesis, CW polysaccharide metabolic processes, cellulose metabolic processes and CW macromolecular metabolic processes (Fig. 4). There were no significantly enriched GO terms associated with CW metabolism found among the upregulated Cd-responsive DEGs and downregulated DSE-responsive DEGs (Fig. 4).

KEGG analyses recovered 15 significantly enriched pathways from the up- and downregulated genes among the 4 comparisons. Four KEGG pathways were associated with key components of CW metabolism involving lignin, cellulose, hemicellulose, and pectin. Heatmaps associated with these 4 KEGG pathways responded to both DSE colonization and Cd stress. Other pathways responded only to DSE colonization or Cd stress. For example, a total of 100 DEGs were related to lignin metabolisms, including 24 genes participating in the biosynthesis of 4 lignin monomers and 76 genes participating in the lignin synthesis, showing different trends. These DEGs were downregulated under the influence of Cd stress ranged from 100 % in non-DSE maize to 79 % in DSE maize, whereas DEGs were downregulated by DSE were only 38 % and 4 %, respectively. In contrast, DEGs were unregulated by DSE were 62 % and 96 % from maize root without and with Cd stress, respectively. Comparable trends were found in the regulation of genes participating in the synthesis of cellulose, hemicellulose, and pectin, as well as the methylation of pectin by DSE or Cd alone. Some genes showed opposite responses to the Cd and DSE treatments. For example, the expression of genes encoding pectinesterase was downregulated by Cd stress, whereas DSE colonization upregulated these genes. These patterns were found in approximately 40 genes related to CW proteins, such as expansins, proline-rich proteins, glycine-rich proteins, cysteine-rich proteins, and arabinogalactan proteins (Fig. 5). Additionally, we also noted that, although a consistent gene expression patterning across the most parallel genes encoding an annotated protein occurred in a given comparison, there were only a limited number of specifically-differential expression patterns, e.g. in contrast to most upregulated DEGs encoding peroxiredoxin 6, 1-Cys peroxiredoxin (EC: 1.11.1.7) in Cd_DSE, while GRMZM2G042347 displayed opposite regulation (downregulated with $\log_{10}$ (FPKM + 1) values from 7.41 in Cd_nDSE to 5.26 in Cd_DSE).

4. Discussion

In recent years, studies have documented not only the remarkable diversity of endophytic fungi colonizing different parts of land plants but also documented various benefits provided by these fungi for the survival of plants in both abiotic and biotic stresses (Brader et al., 2017; Thavamani et al., 2017). These results motivated the proposal of evolutionary correlations between partners of symbiomes replacing the previous paradigm to study the evolution of each organism independently (Tripp et al., 2017). Thus, this study is important because it tests a particular functional prediction of how an endophytic fungal partner supports the resistance of its plant partner. The strength of this study is arguable that it establishes the pathway of how inoculation by DSE affects the ability of plants to resist the toxicity of trace metals (Li et al., 2011). We recommend careful assessments that employ experimental setups for testing predicted modifications of the plant proteome and phenotype caused by endophytic fungi under stress conditions.

The results of the current experiments showed that over 56 % of granular Cd deposits were mainly bound in the CWs of both inoculated and noninoculated maize roots, which was consistent with the knowledge on the preferential binding of Cd to the CWs (Parrotta et al., 2015; Krzesłowska et al., 2019). Importantly, we observed an enhanced sequestration compartment of a Cd subcellular distribution in the root CWs of *E. pisciphila*-colonized maize relative to that in the non-inoculated controls. Several similar modifications of cellular uptake and subcellular distributions of metal ions by mycorrhizal colonization, e.g.,

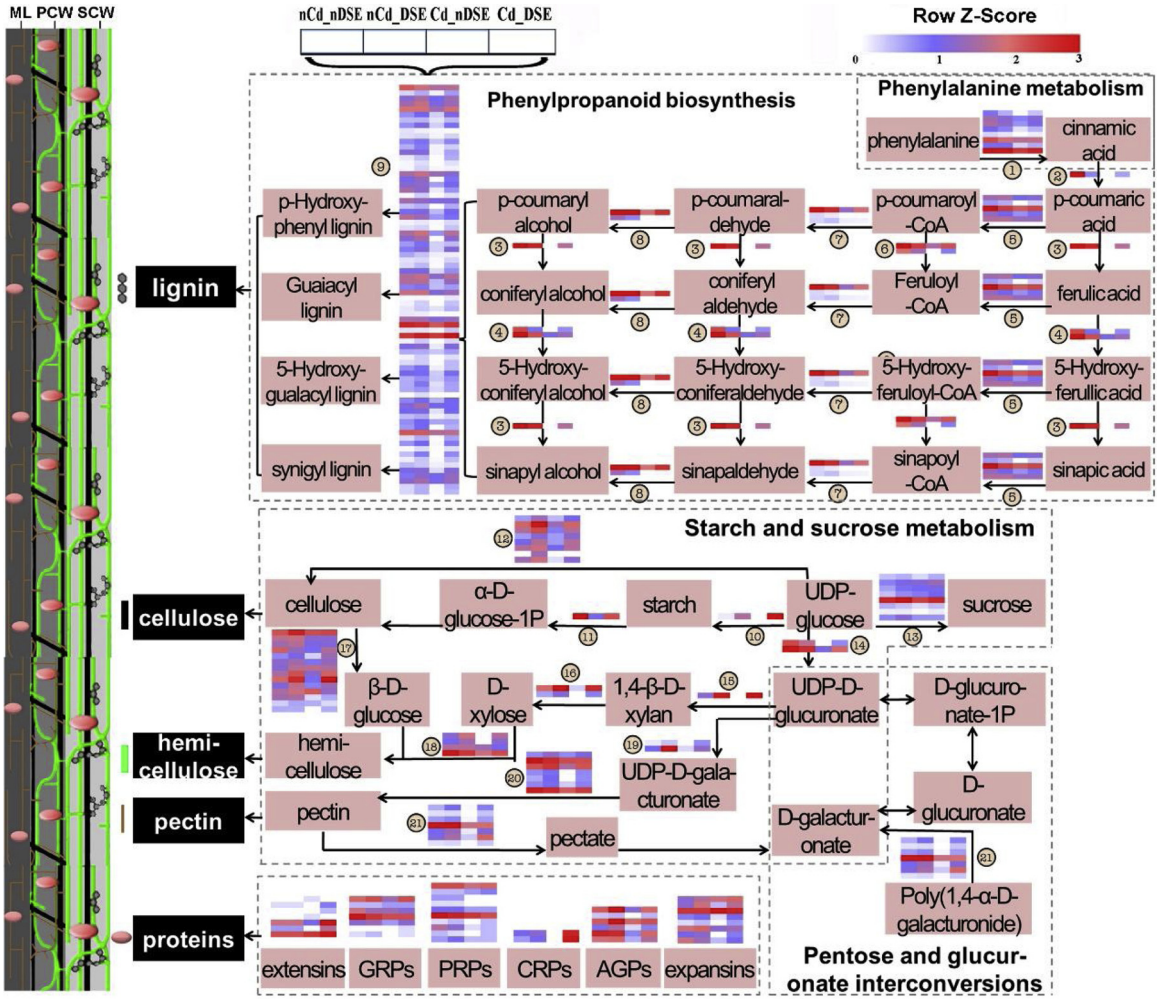

Fig. 5. Transcriptional changes in genes related to CW synthesis pathways responsible for Cd and DSE factors in maize roots among the 4 treatments (i.e. read from left to right in boxes: nCd_nDSE, nCd_DSE, Cd_nDSE and Cd_DSE, respectively). ML, middle lamella; PCW, primary CW; SCW, secondary CW; GRPs, glycine-rich proteins; PRPs, proline-rich proteins; CRPs, cysteine-rich proteins; AGPs, arabinogalactan proteins. ① phenylalanine/tyrosine ammonia lyase [EC: 4.3.1.24, 4.3.1.25]; ② trans-cinnamate 4-monooxygenase [EC:1.14.13.11]; ③ caffeic acid 3-O-methyltransferase [EC:2.1.1.68]; ④ ferulate-5-hydroxylase F5H; ⑤ 4-coumarate–CoA ligase [EC:6.2.1.12]; ⑥ caffeoyl-CoA O-methyltransferase 1 [EC:2.1.1.104]; ⑦ cinnamoyl-CoA reductase [EC:1.2.1.44]; ⑧ cinnamyl-alcohol dehydrogenase [EC:1.1.1.195]; ⑨ peroxiredoxin 6,1-Cys peroxiredoxin [EC:1.11.1.7] and laccase. ⑩ 1,4-alpha-glucan branching enzyme [EC:2.4.1.18]; ⑪ glycogen phosphorylase [EC:2.4.1.1]; ⑫ sucrose synthase [EC:2.4.1.13], sucrose-phosphate synthase [EC:2.4.1.14]; ⑬ UDP glucose 6-dehydrogenase [EC:1.1.1.22]; ⑭ 1,4-beta-D-xylan synthase [EC:2.4.2.24]; ⑮ beta-D-xylosidase 4 [EC:3.2.1.37]; ⑯ endoglucanase [EC:3.2.1.4], beta-glucosidase [EC:3.2.1.21]; ⑰ UDP-glucuronate 4-epimerase [EC:5.1.3.6]; ⑱ alpha-1,4-galacturonosyltransferase [EC:2.4.1.43]; ⑲ pectinesterase [EC:3.1.1.11]. The blue-to-red color transition indicates increasing values of $\log_{10}$ (FPKM +1).

a significantly increased proportions of Pb in the *Robinia pseudoacacia* CWs or Cd and Cu in *Oryza sativa* (Zhang et al., 2009; Li et al., 2016; Huang et al., 2017), further confirmed the vital roles of remodeling CWs in cellular responses to metal stress in plants (Krzesłowska et al., 2019). In fact, the strong capacity for noncovalent and/or covalent metal ion binding and sequestration via the functional groups in CWs, e.g., polysaccharides, lignin, proteins and others of CWs, have been repeatedly observed in numerous plants (Krzesłowska, 2011; Parrotta et al., 2015). FTIR analysis further showed that the *E. pisciphila* colonization changed the peak positions of the polysaccharide chain and sulfate/phosphate groups in pectin and the hydroxyl/amine, carboxyl, and polysaccharide chain groups in hemicellulose 1, which suggested that more Cd ions bound to these functional groups (Riaz et al., 2018; Xia et al., 2018). We argued that the altered cellular and subcellular distribution of metals in maize roots might protect the living protoplasts, relieve metal phytotoxicity in diverse root organelles, and lower the overall translocation of metal ions in plant shoots (via the transpiration stream to the leaves) (Clemens, 2006). Our results revealed that internal detoxification may be achieved through the enhanced cellular/subcellular compartmentalization in CWs bioaugmented by root-associated DSE colonization and may support the first strategy of remodeling root CWs in Cd retention in response to metal entry.

We also found a distinct Cd accumulation pattern in various subfractions of CW, with a significantly increased proportion of Cd accumulated in pectin and hemicellulose 1, but a decrease in hemicellulose 2 and the others in DSE inoculated maize, which in further support of the consequential role of hemicelluloses and pectin, two major polysaccharides that have the ability to bind metal ions in the CWs (Zhu et al., 2017). Similarly, Zhao et al. (2019) also observed that the increasing cadmium retention in root of oilseed rape (*Brassica napus*) by the elevated Cd concentration of pectin and hemicellulose 2 by selenium (Se), contributed to the reduction of Cd uptake in root and therefore transportation to stem, pod, and finally seed.

The ability of DSE colonization to bioaugment the maize roots for Cd accumulation by remodeling the root CWs was further supported by the enhanced activities of key enzymes involved in the CW metabolism of maize root, e.g., PME, CWP, and PAL. We argued that the increased activity of PME by DSE inoculation resulted in the demethylation of CW

pectin, which may generate more negative charges to allow more cation binding (El-Moneim et al., 2014). Additionally, both the enhanced activity of PAL and CWP, as two key enzymes involved with the polymerization of lignin monomers (Passardi et al., 2004; Pawlak-Sprada et al., 2011), contributed to CW remodeling in *E. pisciphila*-colonized maize under Cd stress (Qiu et al., 2018). More importantly, an elevated accumulation of lignin in cell walls could bind multiple heavy metal ions (Cu^{2+}, Cd^{2+}, Pb^{2+}, etc.) by interaction with a large number of functional groups (hydroxyl, carboxyl, methoxyl, etc.) (Liu et al., 2018; Qiu et al., 2018). Subsequently, our RNA-seq analysis also supported the above explanation and found that most genes involved, for instance, pectinesterase genes, encoding the synthesis of lignin, were upregulated for the DSE colonized maize under Cd stress. In addition, Cd stress increased the total activity of CWP, which can be found in a variety of isoforms that differ in their electrophoretic mobilities, e.g. ionic fraction, covalent fraction, intercellular fraction (González et al., 1999). The increased activity of the total CWP in the current study was contradictory to the inhibited activity of both PAL and PME by Cd. In fact, a similar phenomenon was repeatedly reported in numerous plants under different metal stresses (Gall et al., 2015). We argued that the increase of CWP activity caused both by DSE and by Cd may function in response to abiotic stresses or biotic factors, which precisely controlled cell wall loosening and stiffening, and further regulated plant growth and development (Francoz et al., 2015). We also noted that the remodeling cell wall caused by Cd stress did not inhibit DSE colonization, instead of a higher colonization intensity than that in no metal-supplemented controls. While one must keep in mind that a complex and cooperative regulatory network tightly controlling intracellular interaction between plants and DSE is in need of further attention.

The RNA-seq results well verified that DSE colonization remodeled the host plant CWs to alleviate the Cd toxicity of maize, which was consistent with the higher expression of CW related genes in low Cd-accumulating cultivar Fenghua 1 than in Silihong (a high-Cd cultivar) (Yu et al., 2019). For example, GO analysis showed that Cd downregulated genes but DSE upregulated genes were significantly enriched in phenylpropanoid biosynthetic and metabolic process. Interestingly, Feng et al. (2018) also found that the overrepresented phenylpropanoid biosynthesis pathway of *Sorghum bicolor* was induced responses beneficial to counteract Cd stresses, as well as in Arabidopsis root hair (Cao et al., 2019). In fact, the phenylpropanoid biosynthesis pathway generates an enormous array of secondary metabolites, the products of which serve as a metabolite source for lignin biosynthesis (Vogt, 2010; Scully et al., 2016). Thus, the DSE-upregulated phenylpropanoid biosynthesis contributed to the adsorption of metal ions on the lignin surfaces via carboxylic- and phenolic-type surface groups (Guo et al., 2008), which was in accordance with the above physiological results. Furthermore, GO and KEGG analyses of CW-related genes indicated that there was a similar regulation trend in the biosynthesis/modification, e.g., cellulose and hemicellulose, by Cd stress and DSE colonization, respectively. Consequently, the upregulation biosynthesis pathway by DSE resulted in the remodeling of the CWs and contributed to the Cd cellular/subcellular compartmentalization of CWs in plants to lower the entry of trace metals in the protoplast (Vatehová-Vivodová et al., 2018; Jia et al., 2019), thereby conferring the tolerant races of plants that can survive and thrive on metal-contaminated soils. Taken together, these dramatic changes in gene expression and enzymatic activity might have made the DSE remodeling of CWs of the host plant an active player in tackling the challenge imposed by excessive Cd in maize root. Additionally, with rare exceptions, the functional roles of the parallel genes with a distinct regulation e.g. the downregulated gene GRMZM2G042347 by DSE in the comparison of Cd_nDSE vs. Cd_DSE are needed to further be evaluated.

Evidence accumulated in recent years supports the crucial role of remodeled CWs in enabling plants to adapt to environmental challenges (Parrotta et al., 2015). The novelty of our research is the first analysis characterizing the specific physiological, biochemical and molecular response of plant CWs bioaugmented by their root-associated DSE to substrate with an extremely high concentration of toxic Cd, which enables the tolerant races of plants that can survive and thrive on metal-contaminated soils. Obviously, the enhanced tolerant races of plants are attributed to the interaction between host and microbiome together (Thijs et al., 2016), which are beneficial from the enhanced Cd binding both by the remodeling cell walls of plants as well as the root-colonizing intercellular DSE hyphae and microsclerotia. Particular emphasis needs to further explore the functional roles and response of the altered cell wall components by DSE e.g. lignin, pectin, which was confirmed by the definitive evidence from the global transcriptome analysis, including the altered levels of CW components, the cadmium kinetics, molecular biosynthetic pathways and etc. (Qiu et al., 2018; Jia et al., 2019). This is arguably one of the first studies exploring the economic potential of plant-endophytic plant interactions by elucidating the mechanisms of how DSEs transform the CW matrix to immobilize toxic metal ions. This study demonstrated the potential of the utilization of endophytic fungi to promote the spontaneous establishment of mine plant species as well as phytostabilization via the sequestration of metals within the rhizosphere and plant tissues (Mendez and Maier, 2008).

Data availability

All datasets generated for this study are included in the manuscript.

Author contributions

M.S., T.L., and Z.Z. conceived and designed the research in general. M.S., R.X., and G.C. performed the experiments. M.S., H.S., T.L., H.Z., and Z.Z. performed the analyses and wrote the paper. Correspondence and requests for materials should be addressed to T.L. or Z.Z.

Author statement

Mi Shen: Conceptualization, Methodology, Writing - Original Draft, Investigation. **Harald Schneider:** Writing - Review & Editing. **Runbing Xu:** Software, Formal analysis. **Guanhua Cao:** Software, Formal analysis. **Hanbo Zhang:** Formal analysis. **Tao Li:** Conceptualization, Writing - Review & Editing, Project administration, Funding acquisition. **Zhiwei Zhao:** Conceptualization, Writing - Review & Editing, Supervision, Funding acquisition

Funding

This study was financially supported by Yunnan Provincial Science and Technology Department-Yunnan University Joint Foundation, the key project (2018FY001(-010)) and National Natural Science Foundation of China (41761106, 41461073 and 31460114).

Declaration of Competing Interest

The authors declare no competing financial interests.

Acknowledgments

We are grateful to Prof. Yunsu Shi (Institute of Crop Sciences, Chinese Academy of Agricultural Sciences) for providing the maize B73 seeds. The authors gratefully acknowledge Dr. Fangdong Zhan (College of Resources and Environment, Yunnan Agricultural University, PR China) for his help in metal analysis.

Appendix A. Supplementary data

Supplementary material related to this article can be found, in the online version, at doi:https://doi.org/10.1016/j.envexpbot.2020.104000.

References

Anders, S., Pyl, P.T., Huber, W., 2015. HTSeq–a Python framework to work with high-throughput sequencing data. Bioinformatics 31, 166–169.

Bacon, M.A., Thompson, D.S., Davies, W.J., 1997. Can cell wall peroxidase activity explain the leaf growth response of *Lolium temulentum* L. during drought? J. Exp. Bot. 48, 2075–2085.

Berni, R., Luyckx, M., Xu, X., Legay, S., Sergeant, K., Hausman, J.F., et al., 2019. Reactive oxygen species and heavy metal stress in plants: impact on the cell wall and secondary metabolism. Environ. Exp. Bot. 161, 98–106.

Brader, G., Compant, S., Vescio, K., Mitter, B., Trognitz, F., Ma, L.J., et al., 2017. Ecology and genomic insights on plant-pathogenic and plant-nonpathogenic endophytes. Annu. Rev. Phytopathol. 55, 61–83.

Cahill, D.M., Mccomb, J.A., 1992. A comparison of changes in phenylalanine ammonia-lyase activity, lignin and phenolic synthesis in the roots of *Eucalyptus calophylla* (field resistant) and *E. marginata* (susceptible) when infected with *Phytophthora cinnamomi*. Physiol. Mol. Biol. Plants 40, 315–332.

Cao, J.Y., Ye, C.T., Hao, G.J., Dabney-Smith, C., Hunt, A.G., Li, Q.Q., 2019. Root hair single cell type specific profiles of gene expression and alternative polyadenylation under cadmium stress. Front. Plant Sci. 10, 589. https://doi.org/10.3389/fpls.2019.00589.

Chen, K., Fessehaie, A., Arora, R., 2012. Selection of reference genes for normalizing gene expression during seed priming and germination using qPCR in *Zea mays* and *Spinacia oleracea*. Plant Mol. Biol. Rep. 30, 478–487.

Clemens, S., 2006. Toxic metal accumulation, responses to exposure and mechanisms of tolerance in plants. Biochimie 88, 1707–1719.

Douchiche, O., Driouich, A., Morvan, C., 2010. Spatial regulation of cell-wall structure in response to heavy metal stress: cadmium-induced alteration of the methyl-esterification pattern of homogalacturonans. Ann. Bot. 105, 481–491.

El-Moneim, D.A., Contreras, R., Silva-Navas, J., Gallego, F.J., Figueiras, A.M., Benito, C., 2014. Pectin methylesterase gene and aluminum tolerance in *Secale cereale*. Environ. Exp. Bot. 107, 125–133.

Feng, J., Jia, W., Lv, S., Bao, H., Miao, F., Zhang, X., et al., 2018. Comparative transcriptome combined with morpho-physiological analyses revealed key factors for differential cadmium accumulation in two contrasting sweet sorghum genotypes. Plant Biotechnol. J. 16, 558–571.

Fernandez, R., Fernandez-Fuego, D., Bertrand, A., Gonzalez, A., 2014. Strategies for Cd accumulation in *Dittrichia viscosa* (L.) Greuter: role of the cell wall, non-protein thiols and organic acids. Plant Physiol. Biochem. 78, 63–70.

Francoz, E., Ranocha, P., Nguyen-Kim, H., Jamet, E., Burlat, V., Dunand, C., 2015. Roles of cell wall peroxidases in plant development. Phytochemistry 112, 15–21.

Gall, H.L., Philippe, F., Domon, J.M., Gillet, F., Pelloux, J., Rayon, C., 2015. Cell wall metabolism in response to abiotic stress. Plants 4, 112–166.

González, L.F., Perez, F., Rojas, M.C., 1999. Indole-3-acetic acid control on acidic Oat cell wall peroxidases. J. Plant Growth Regul. 18, 25–31.

Guo, X., Zhang, S., Shan, X.Q., 2008. Adsorption of metal ions on lignin. J. Hazard. Mater. 151, 134–142.

Hou, D., Wang, K., Liu, T., Wang, H., Lin, Z., Qian, J., et al., 2017. Unique rhizosphere micro-characteristics facilitate phytoextraction of multiple metals in soil by the hyperaccumulating plant *Sedum alfredii*. Environ. Sci. Technol. 51, 5675–5684.

Huang, L., Zhang, H., Song, Y., Yang, Y., Chen, H., Tang, M., 2017. Subcellular compartmentalization and chemical forms of lead participate in lead tolerance of *Robinia pseudoacacia* L. with *Funneliformis mosseae*. Front. Plant Sci. 8, 517. https://doi.org/10.3389/fpls.2017.00517.

Jia, H., Wang, X., Wei, T., Zhou, R., Muhammad, H., Hua, L., et al., 2019. Accumulation and fixation of Cd by tomato cell wall pectin under Cd stress. Environ. Exp. Bot. 167, 103829.

Kollárová, K., Kusá, Z., Vatehová-Vivodová, Z., Lišková, D., 2019. The response of maize protoplasts to cadmium stress mitigated by silicon. Ecotoxicol. Environ. Saf. 170, 488–494.

Krzesłowska, M., 2011. The cell wall in plant cell response to trace metals: polysaccharide remodeling and its role in defense strategy. Acta Physiol. Plant. 33, 35–51.

Krzesłowska, M., Timmers, A.C.J., Mleczek, M., Niedzielski, P., Rabęda, I., Woźny, A., et al., 2019. Alterations of root architecture and cell wall modifications in *Tilia cordata* Miller (Linden) growing on mining sludge. Environ. Pollut. 248, 247–259.

Lan, X.Y., Yan, Y.Y., Yang, B., Li, X.Y., Xu, F.L., 2019. Subcellular distribution of cadmium in a novel potential aquatic hyperaccumulator - *Microsorum pteropus*. Environ. Pollut. 248, 1020–1027.

Li, T., Liu, M.J., Zhang, X.T., Zhang, H.B., Sha, T., Zhao, Z.W., 2011. Improved tolerance of maize (*Zea mays* L.) to heavy metals by colonization of a dark septate endophyte (DSE) *Exophiala pisciphila*. Sci. Total Environ. 409, 1069–1074.

Li, H., Luo, N., Zhang, L.J., Zhao, H.M., Li, Y.W., Cai, Q.Y., et al., 2016. Do arbuscular mycorrhizal fungi affect cadmium uptake kinetics, subcellular distribution and chemical forms in rice? Sci. Total Environ. 571, 1183–1190.

Liu, Q., Luo, L., Zheng, L., 2018. Lignins: biosynthesis and biological functions in plants. Int. J. Mol. Sci. 19, 335. https://doi.org/10.3390/ijms19020335.

Mendez, M.O., Maier, R.M., 2008. Phytostabilization of mine tailings in arid and semiarid environments—an emerging remediation technology. Environ. Health Persp. 116, 278–283.

Moreira, H., Pereira, S.I.A., Marques, A.P.G.C., Rangel, A.O.S.S., Castro, P.M.L., 2016. Selection of metal resistant plant growth promoting rhizobacteria for the growth and metal accumulation of energy maize in a mine soil — effect of the inoculum size. Geoderma 278, 1–11.

Muschitz, A., Riou, C., Mollet, J.C., Gloaguen, V., Faugeron, C., 2015. Modifications of cell wall pectin in tomato cell suspension in response to cadmium and zinc. Acta Physiol. Plant. 37, 245. https://doi.org/10.1007/s11738-015-2000-y.

Parrotta, L., Guerriero, G., Sergeant, K., Cai, G., Hausman, J.F., 2015. Target or barrier? The cell wall of early- and later-diverging plants vs cadmium toxicity: differences in the response mechanisms. Front. Plant Sci. 6, 133. https://doi.org/10.3389/fpls.2015.00133.

Passardi, F., Penel, C., Dunand, C., 2004. Performing the paradoxical: how plant peroxidases modify the cell wall. Trends Plant Sci. 9, 534–540.

Pawlak-Sprada, S., Arasimowicz-Jelonek, M., Podgórska, M., Deckert, J., 2011. Activation of phenylpropanoid pathway in legume plants exposed to heavy metals. Part I. Effects of cadmium and lead on phenylalanine ammonia-lyase gene expression, enzyme activity and lignin content. Acta Biochim. Pol. 58, 211–216.

Peng, J.S., Wang, Y.J., Ding, G., Ma, H.L., Zhang, Y.J., Gong, J.M., 2017. A pivotal role of cell wall in cadmium accumulation in the Crassulaceae hyperaccumulator *Sedum plumbizincicola*. Mol. Plant 10, 771–774.

Qiao, X., Zheng, Z., Zhang, L., Wang, J., Shi, G., Xu, X., 2015. Lead tolerance mechanism in sterilized seedlings of *Potamogeton crispus* L.: subcellular distribution, polyamines and proline. Chemosphere 120, 179–187.

Qiu, W., Song, X., Han, X., Liu, M., Qiao, G., Zhuo, R., 2018. Overexpression of *Sedum alfredii* cinnamyl alcohol dehydrogenase increases the tolerance and accumulation of cadmium in Arabidopsis. Environ. Exp. Bot. 155, 566–577.

Quinlan, A.R., Hall, I.M., 2010. BEDTools: a flexible suite of utilities for comparing genomic features. Bioinformatics 26, 841–842.

Riaz, M., Yan, L., Wu, X., Hussain, S., Aziz, O., Imran, M., et al., 2018. Boron reduces aluminum-induced growth inhibition, oxidative damage and alterations in the cell wall components in the roots of trifoliate orange. Ecotoxicol. Environ. Saf. 153, 107–115.

Schnable, P.S., Ware, D., Fulton, R.S., Stein, J.C., Wei, F., Pasternak, S., et al., 2009. The B73 maize genome: complexity, diversity, and dynamics. Science 326, 1112–1115.

Scully, E.D., Gries, T., Sarath, G., Palmer, N.A., Baird, L., Serapiglia, M.J., et al., 2016. Overexpression of *SbMyb60* impacts phenylpropanoid biosynthesis and alters secondary cell wall composition in *Sorghum bicolor*. Plant J. 85, 378–395.

Shi, W., Zhang, Y., Chen, S., Polle, A., Rennenberg, H., Luo, Z.B., 2019. Physiological and molecular mechanisms of heavy metal accumulation in nonmycorrhizal versus mycorrhizal plants. Plant Cell Environ. 42, 1087–1103.

Slycken, S.V., Witters, N., Meers, E., Peene, A., Michels, E., Adriaensen, et al., 2013. Safe use of metal-contaminated agricultural land by cultivation of energy maize (*Zea mays*). Environ. Pollut. 178, 375–380.

Thavamani, P., Samkumar, R.A., Satheesh, V., Subashchandrabose, S.R., Ramadass, K., Naidu, R., et al., 2017. Microbes from mined sites: harnessing their potential for reclamation of derelict mine sites. Environ. Pollut. 230, 495–505.

Thewys, T., Witters, N., Meers, E., Vangronsveld, J., 2010. Economic viability of phytoremediation of a cadmium contaminated agricultural area using energy maize. Part II: Economics of anaerobic digestion of metal contaminated maize in Belgium. Int. J. Phytoremediat. 12, 663–679.

Thijs, S., Sillen, W., Rineau, F., Weyens, N., Vangronsveld, J., 2016. Towards an enhanced understanding of plant-microbiome interactions to improve phytoremediation: engineering the metaorganism. Front. Microbiol. 7, 341. https://doi.org/10.3389/fmicb.2016.00341.

Trapnell, C., Williams, B.A., Pertea, G., Mortazavi, A., Kwan, G., van Baren, M.J., et al., 2010. Transcript assembly and quantification by RNA-Seq reveals unannotated transcripts and isoform switching during cell differentiation. Nat. Biotechnol. 28, 511–515.

Tripp, E.A., Zhang, N., Schneider, H., Huang, Y., Mueller, M., Hu, Z., et al., 2017. Reshaping Darwin' s tree: impact of the symbiome. Trends Ecol. Evol. 32, 552–555.

Vatehová-Vivodová, Z., Kollárová, K., Malovíková, A., Lišková, D., 2018. Maize shoot cell walls under cadmium stress. Environ. Sci. Pollut. Res. Int. 25, 22318–22322.

Vogt, T., 2010. Phenylpropanoid biosynthesis. Mol. Plant 3, 2–20.

Voxeur, A., Hofte, H., 2016. Cell wall integrity signaling in plants: "To grow or not to grow that's the question". Glycobiology 26, 950–960.

Wang, J.L., Li, T., Liu, G.Y., Smith, J.M., Zhao, Z.W., 2016. Unraveling the role of dark septate endophyte (DSE) colonizing maize (*Zea mays*) under cadmium stress: physiological, cytological and genic aspects. Sci. Rep. 6, 22028. https://doi.org/10.1038/srep22028.

Wu, J., Guo, J., Hu, Y., Gong, H., 2015. Distinct physiological responses of tomato and cucumber plants in silicon-mediated alleviation of cadmium stress. Front. Plant Sci. 6, 453. https://doi.org/10.3389/fpls.2015.00453.

Xia, Y., Yin, S., Zhang, K., Shi, X., Lian, C., Zhang, H., et al., 2018. OsWAK11, a rice wall-associated kinase, regulates Cu detoxification by alteration the immobilization of Cu in cell walls. Environ. Exp. Bot. 150, 99–105.

Xiong, J., An, L.Y., Lu, H., Zhu, C., 2009. Exogenous nitric oxide enhances cadmium tolerance of rice by increasing pectin and hemicellulose contents in root cell wall. Planta 230, 755–765.

Yang, L.T., Liu, J.W., Wu, Y.M., Qi, Y.P., Wang, J.L., Lai, N.W., et al., 2018. Proteome profile analysis of boron-induced alleviation of aluminum-toxicity in *Citrus grandis* roots. Ecotoxicol. Environ. Saf. 162, 488–498.

Yu, R.G., Ma, Y.Y., Li, Y., Li, X., Liu, C.F., Du, X.L., et al., 2019. Comparative transcriptome analysis revealed key factors for differential cadmium transport and retention in roots of two contrasting peanut cultivars. BMC Genomics 19, 938. https://doi.org/10.1186/s12864-018-5304-7.

Zhang, X.H., Lin, A.J., Gao, Y.L., Reid, R.J., Wong, M.H., Zhu, Y.G., 2009. Arbuscular mycorrhizal colonisation increases copper binding capacity of root cell walls of *Oryza sativa* L. and reduces copper uptake. Soil Biol. Biochem. 41, 930–935.

Zhang, Y., Li, T., Zhao, Z.W., 2013. Colonization characteristics and composition of dark septate endophytes (DSE) in a lead and zinc slag heap in southwest China. Soil Sediment Contam. 22, 532–545.

Zhang, Z.C., Zhou, H., Yu, Q., Li, Y., Mendoza-Cozatl, D.G., Qiu, B., et al., 2017.

Quantitative proteomics analysis of leaves from two *Sedum alfredii* (Crassulaceae) populations that differ in cadmium accumulation. Proteomics 17, 10. https://doi.org/10.1002/pmic.201600456.

Zhang, J., Qian, Y., Chen, Z., Amee, M., Niu, H., Du, D., et al., 2019a. Lead-induced oxidative stress triggers root cell wall remodeling and increases lead absorption through esterification of cell wall polysaccharide. J. Hazard. Mater. https://doi.org/10.1016/j.jhazmat.2019.121524.

Zhang, X.F., Hu, Z.H., Yan, T.X., Lu, R.R., Peng, C.L., Li, S.S., et al., 2019b. Arbuscular mycorrhizal fungi alleviate Cd phytotoxicity by altering Cd subcellular distribution and chemical forms in *Zea mays*. Ecotoxicol. Environ. Saf. 171, 352–360.

Zhao, L., Li, T., Yu, H., Chen, G., Zhang, X., Zheng, Z., et al., 2015. Changes in chemical forms, subcellular distribution, and thiol compounds involved in Pb accumulation and detoxification in *Athyrium wardii* (Hook.). Environ. Sci. Pollut. Res. 22, 12676–12688.

Zhao, Y., Hu, C., Wu, Z., Liu, X., Cai, M., Jia, W., et al., 2019. Selenium reduces cadmium accumulation in seed by increasing cadmium retention in root of oilseed rape (*Brassica napus* L.). Environ. Exp. Bot. 158, 161–170.

Zhong, H., Lauchli, A., 1993. Changes of cell wall composition and polymer size in primary roots of cotton seedlings under high salinity. J. Exp. Bot. 44, 773–778.

Zhu, X.F., Wan, J.X., Wu, Q., Zhao, X.S., Zheng, S.J., Shen, R.F., 2017. PARVUS affects aluminium sensitivity by modulating the structure of glucuronoxylan in *Arabidopsis thaliana*. Plant Cell Environ. 40, 1916–1925.